Journal of Radiation Research and Applied Sciences 17 (2024) 100924

Contents lists available at ScienceDirect

Journal of Radiation Research and Applied Sciences

journal homepage: www.journals.elsevier.com/journal-of-radiation-research-and-applied-sciences

Investigation of the mechanical and physical properties of mesoporous silicon dioxide fillet epoxy composites

Sinan Köse

Tarsus University, Vocational School of Technical Sciences at Mersin Tarsus Organized Industrial Zone, Department of Machinery and Metal Technologies, 33100, Mediterranean, Mersin, Turkey

ARTICLE INFO

Keywords:
Epoxy composites
Mesoporous silicon dioxide
Nano filler
Mechanical properties

ABSTRACT

In this study, the effect of mesoporous silicon dioxide (M-SiO_2) additives with different surface areas and pore diameters on the morphological and mechanical properties of epoxy composites was investigated. For this purpose, M-SiO_2 particles with different pore diameters and surface areas were synthesized from polyethylene glycol (PEG) with three different molecular weights (PEG2000 (PEG2), PEG6000 (PEG6), and PEG35000 (PEG35) kDa) using the one-step sol-gel technique. The mixing of epoxy resin, hardener and M-SiO_2 fillers, was carried out in a mould followed by using ultrasonic bath and mechanical stirrer.

The mechanical properties of the composites, including hardness, tensile strength, elongation at break, and modulus of elasticity, were studied. FT-IR spectra and XRD patterns show that M-SiO_2 is distributed homogeneously in the epoxy. The epoxy/PEG35M-SiO_2 composites' tensile strength (8.7%) and modulus of elasticity (23.3%) increased with the addition of PEG35M-SiO_2, however their elongation at break (5.1%) decreased.

1. Introduction

Polymer nanocomposites have gained popularity in recent years because of their advantages, such as low cost, easy shaping, and lightness. They can provide improvements in the materials they are used in, such as improvements in mechanical properties, flame retarder, magnetism, and thermal properties. The improvement of these required properties depends on factors such as synthesis technique, particle distribution, and particle size (Fu et al., 2008; Hussain et al., 2006; Kango et al., 2013; Liu et al., 2022; Vaia & Maguire, 2007). Among these structures, nanoscale mesoporous silica, which is especially preferred for use in technological and biomedical applications, is a good candidate (Centi et al., 2009; Cheng et al., 2006; Fowler et al., 2001; Nooney et al., 2002).

Different pore shapes and pore sizes according to the desired dimensions enable the use of mesoporous materials in various applications, such as chromatographic materials. The ability to confine various organic and inorganic materials into porous structures enables usage areas and scientific research to become widespread day by day (Kalita & Kumar, 2007; Shiju et al., 2011; Yoshina-Ishii et al., 1999; Zhao et al., 1998). Previous investigations have shown that the use of polymer composites particularly mesoporous silica as additive materials has shown encouraging results. Homogeneous pore structures and adjustable pore sizes exhibit structural advantages over nanomaterials, and research focuses on how to take advantage of these advantages (Zhang et al., 2010). Based on research, the compatibility and interactions between mesoporous materials and polymer matrixes are the most critical elements. This interaction and compatibility affect the penetration of more polymer chains into the porous structure, thus improving the mechanical and thermal properties (Suzuki, Kiba, & Yamauchi, 2011).

Limited studies exist in the literature on the effects of different pore sizes and volumes on mesoporous polymer matrix composites (Dubey et al., 2015; Suzuki, Kiba, Kamachi, et al., 2011; Ulusal, 2024). Therefore, this study aimed to investigate the effect of mesoporous silicon dioxide (M-SiO2) with different surface area and pore diameter as a 10% additive on the morphological and mechanical properties of epoxy resin matrix composite materials.

2. Materials and methods

Epoxy resin (EPR) produced by Verpol Company, Istanbul, Turkey. Density of EPR is 1.09 g/cm^3. EPR and its hardener are liquid form. The addition was made at ambient temperature with a 1:4 wt ratio of hardener to epoxy.

Sigma Aldrich brand compounds PEG2000, PEG6000, and

E-mail address: sinankose@tarsus.edu.tr.

https://doi.org/10.1016/j.jrras.2024.100924
Received 26 February 2024; Accepted 19 April 2024
Available online 23 April 2024
1687-8507/© 2024 Published by Elsevier B.V. on behalf of The Egyptian Society of Radiation Sciences and Applications. This is an open access article under the CC BY-NC-ND license (http://creativecommons.org/licenses/by-nc-nd/4.0/).

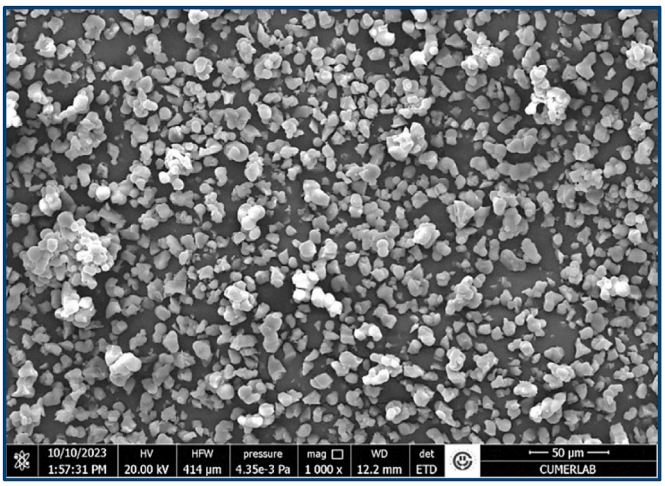


Fig. 1. SEM imagine of M- SiO_2 powder.

PEG35000 were utilized. These compounds were polyethylene glycol flakes with densities of 1.21, 1.20, and 0.5 g/cm3 and molecular weights of 2000, 6000, and 35,000 g/mol. Sigma Aldrich also provided compounds of hydrochloric acid %37, with a density of 1.2 g/cm3, and tetraethyl orthosilicate (TEOS) %98, with a density of 0.933 g/cm3. No additional purification was required for any of the components.

2.1. Preparation of mesoporous SiO_2

A one-step sol-gel synthesis technique was used to prepare mesoporous SiO_2 (Ulusal et al.). For this purpose, 24 g of three different polyethylene glycol compounds (PEG2000, PE6000, and PEG35000) were taken and added to the mixture containing 75 mL of HCl and 220 mL of pure water. 20 mL of the tetraethoxy orthosilicate compound was added and stirred for 24 h at 60 °C and 60 h at 80 °C after the mixture had been thoroughly mixed until transparent. At the end of this period, centrifugation was performed, and the resulting product was washed with pure water until pH 7. After drying in an oven at 70 °C and 24 h, it was calcined in a muffle furnace heated to 550 °C with 15 °C increments per minute and was kept for 6 h. The obtained product was analyzed with XRD, SEM, and FT-IR devices. Fig. 1 shows the SEM image of the produced mesoporous -SiO_2 (M- SiO_2) powder.

2.2. Preparation of M-SiO_2 added epoxy composite

60 mL of epoxy was placed in a container, and M-SiO_2 was added to it, amounting to 10% of the total composite volume. This mixture was mixed first in an ultrasonic bath for 30 min and then via mechanical stirrer for 30 min at 250 rpm.

The mixing ratio of epoxy to hardener chemical was set at 1:4 wt. The M-SiO_2 fillers were separately added to the epoxy at nano filler loadings of 10 vol%. Each resulting mixture of epoxy and M-SiO_2 was stirred for approximately 30 min at 250 rpm with an ultrasonic bath. The mixture was vacuumed for approximately 30 min at room temperature to remove bubbles. The hardener chemical was added, and the mixture was stirred for 250 rpm for 10 min. After mixing at 250 rpm for 7 min, it was poured into dog-bone-shaped moulds with the help of a dropper. After waiting for 24 h, it was removed and tested without any further processing.

4 different samples were obtained, which were evaluated by the study. These samples are pure epoxy composite, PEG2M-SiO_2 filler composite, PEG6M-SiO_2 filler composite and PEG35M-SiO_2 filler composite.

The crystal properties of M-SiO_2 and composites were analyzed using a PANalytical brand Empyrean model XRD device. A FEI Quanta 650

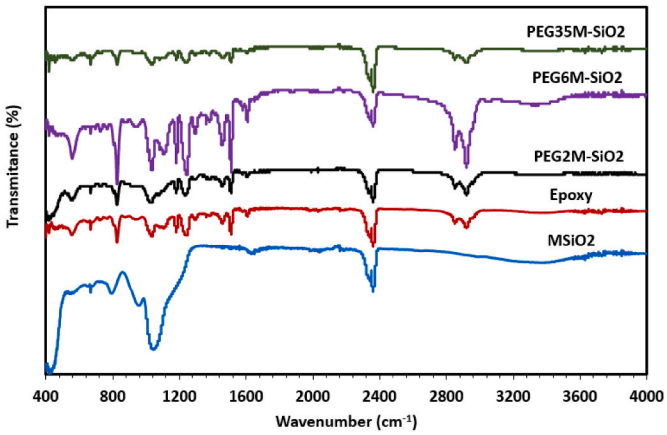


Fig. 2. FT-IR spectra of composites made of epoxy, M-SiO_2, and PEG_xM-SiO_2.

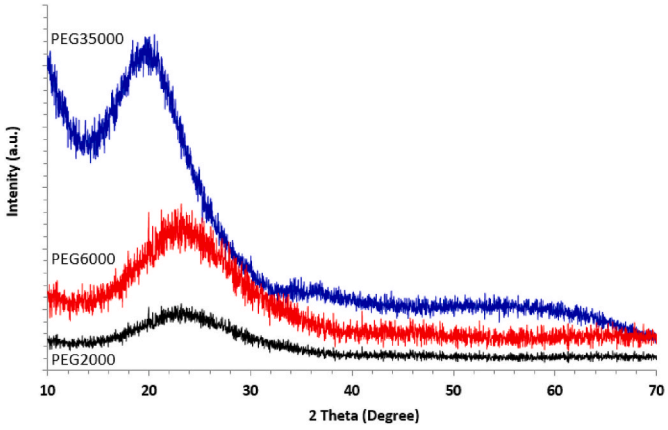


Fig. 3. XRD diffraction patterns of PEG2000, PEG6000, and PEG35000.

Field Emission SEM and an elemental analysis Bruker X Flash 6I30 brand EDS devices were used to observe the homogeneous distribution of M-SiO_2 in epoxy and to examine the surface morphology. Fourier Transform Infrared Spectrophotometer (FT-IR) analysis of all materials was performed on the Thermo Scientific Nicolet IS10 device at 400–4000 cm-1 frequency with diamond ATR. Tensile tests were prepared in accordance with the ASTM D638 standard. The tests were carried out on a Zwick brand Z020 model tensile tester. Each tensile test sample was averaged after being measured at least five times. Tensile tests were carried out at a tensile speed of 10 mm/min.

3. Results and discussion

Fig. 2 shows the FT-IR spectra of M-SiO_2 (synthesized from PEG6), pure epoxy, PEG2M-SiO_2, PEG6M-SiO_2, and PEG35M-SiO_2 composites. When the spectrum of M-SiO_2 is examined, the main Si–O peak at 1070 cm^{-1}, the peak at 1650, and the wide and broad peak between 3000 and 3600 indicate the naturally occurring O–H bond on the SiO_2 surface. The peaks at 772 cm^{-1} and 416 cm^{-1} indicate Si–O–Si bonds (Dubey et al., 2015). Examining the pure epoxy's FT-IR spectrum reveals that the aromatic ring's C=C peaks are located at 1470 and 1510 cm^{-1}, while the aliphatic C–H groups in the epoxy structure are indicated by the peaks at 2800-2950 cm^{-1}. Examining the FT-IR spectra of the composites made by incorporating M-SiO_2 with various pore sizes into the epoxy resin, it is evident that the peaks associated with epoxy are highly prominent because the composite contains 90% epoxy resin. However, it is seen that the most dominant peak of M-SiO_2 causes shifts in the composites. The presence of epoxy peaks in the same region as Si–O prevents this

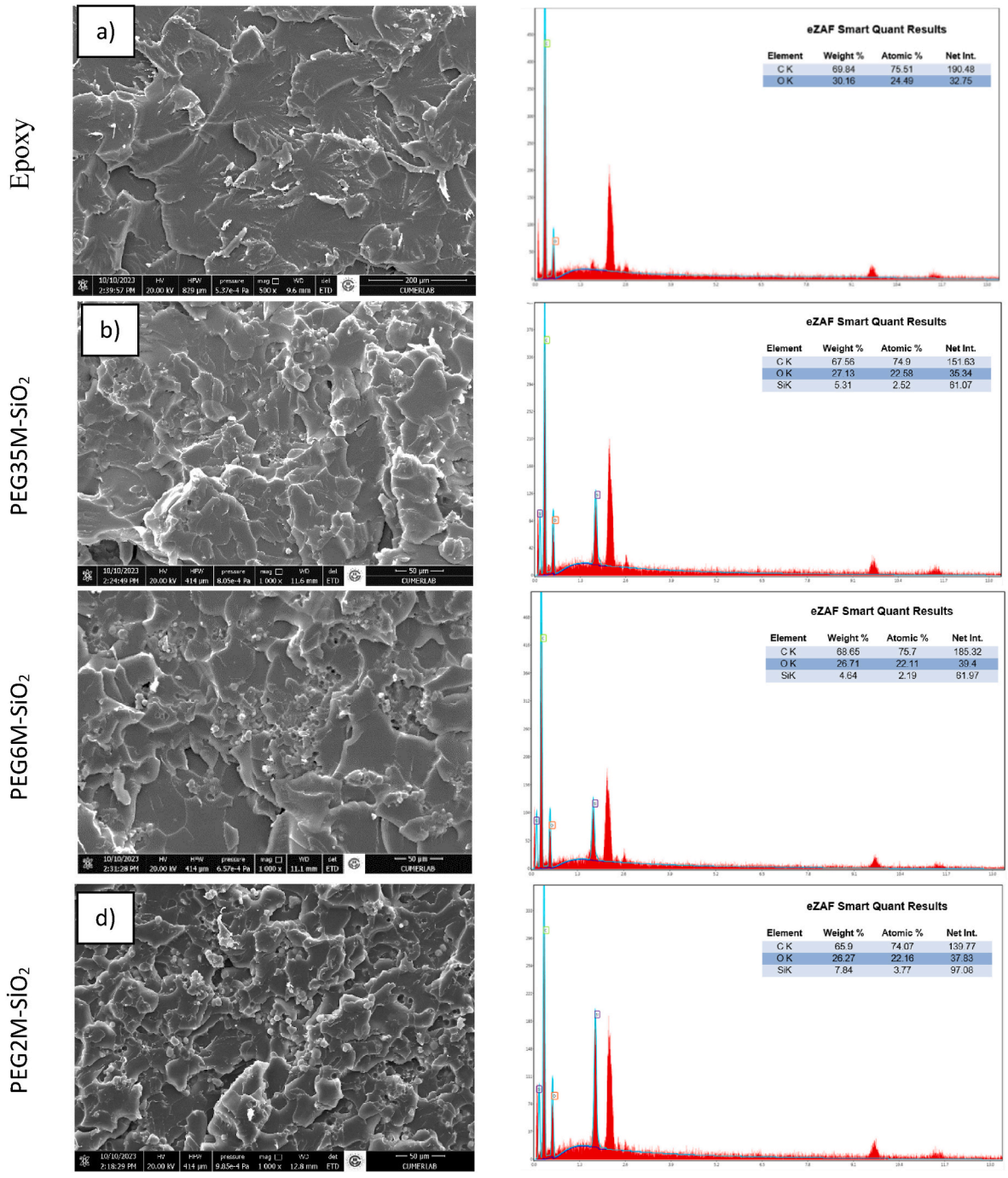


Fig. 4. SEM images and EDS analysis results of fractured surfaces of epoxy and epoxy/PEG$_x$M-SiO$_2$ composites.

peak from becoming evident. However, it is seen that this peak is more prominent in PEG2M-SiO$_2$ than the others. It is also seen that the Si–O–Si peak at 416 cm^{-1} is observed only in PEG2M-SiO$_2$. The reason why silica peaks are more prominent in PEG2M-SiO$_2$ compared to others may be due to the fact that it is less homogeneously distributed than other composites. An increase in the regional proportion of silica will cause it to appear more clearly in the spectrum. All three composites' spectra show that these peaks are not very noticeable, which suggests that the silica is dispersed quite evenly.

Fig. 3 shows the XRD diffraction graphs of PEG2000, PEG6000, and PEG35000. When the XRD diffraction patterns of the prepared mesoporous SiO$_2$ nanoparticles were examined, the main peaks of amorphous SiO$_2$ were obtained in the range of 2θ: 13-38°. As the peaks in the XRD spectrum become sharper and the intensity value increases, this indicates that the substance is moving towards the crystal structure. It is possible to conclude from this data that the M-SiO$_2$ derived from PEG35000 has a more crystalline structure than the others. Since M-SiO$_2$ synthesis is required in this study, the presence of amorphous SiO$_2$ is preferred rather than crystalline SiO$_2$. When the XRD spectrum is compared with studies in the literature, it can be said that the desired structure is obtained (Ulusal et al.).

SEM analyses of epoxy composites with M-SiO$_2$ added and pure epoxy were carried out; the results were shown in Fig. 4. M-SiO$_2$ plays a significant function in the epoxy resin's dispersion state because it allows for mechanical modification of the epoxy. It can be seen from Fig. 4 b-d that M-SiO$_2$ is well dispersed in epoxy. Brittle surface fractures of

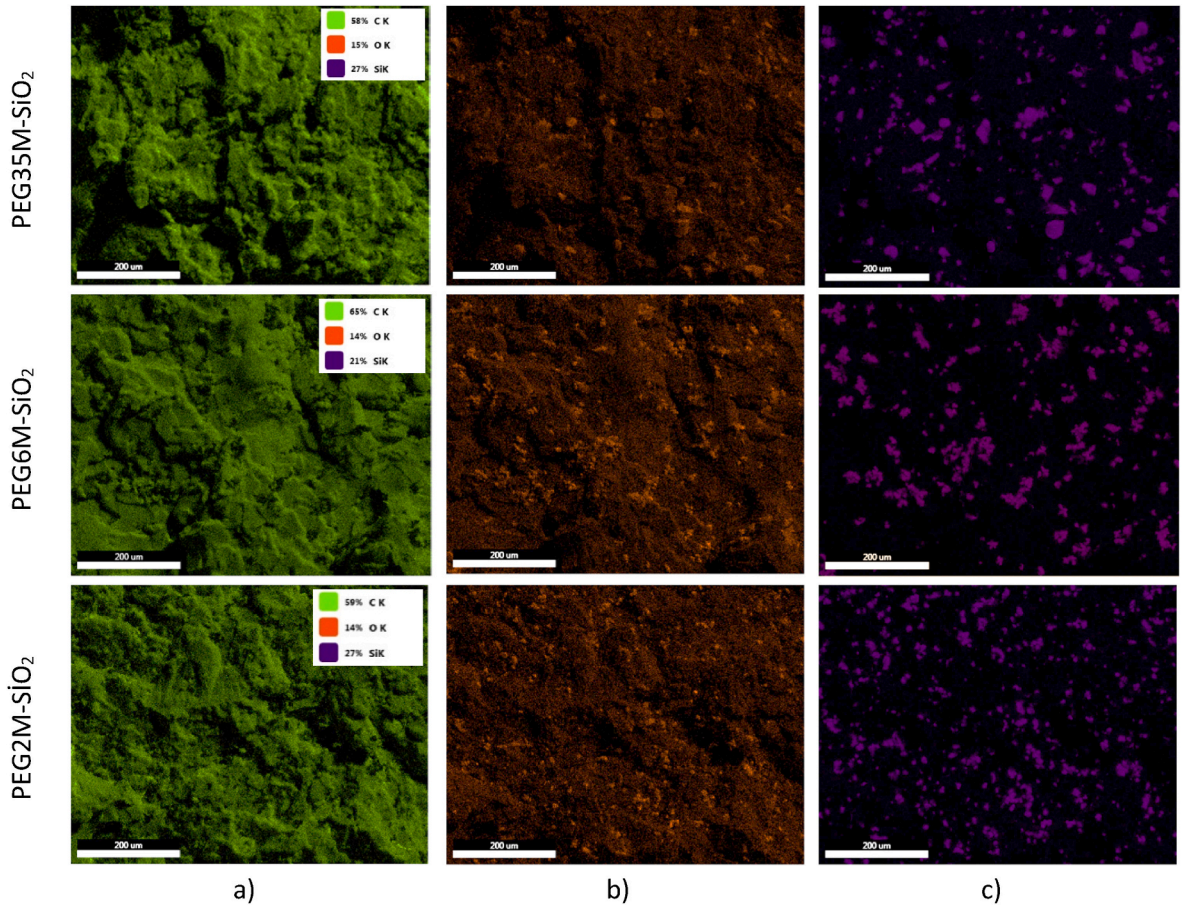


Fig. 5. FE-SEM elemental mapping M-SiO_2 filled epoxy composite a) C, b) O and c) Si distribution.

epoxy and composites occurred in all samples. It has been observed that there is good adhesion between epoxy and M-SiO_2, Despite the partial gaps between epoxy and M-SiO_2, excellent adhesion has been observed between them. It is seen that the M-SiO_2 added to the epoxy matrix in the PEG35M-SiO_2 composite is completely bonded, and there is no independent M-SiO_2 in the epoxy matrix. It is also observed that in PEG6M-SiO_2 and PEG6M-SiO_2 composites, there is M-SiO_2 that has broken off from the epoxy and is not mechanically bonded. When EDS analyzes are evaluated, carbon (C) and oxygen (O) elements are seen in pure epoxy resin. The silicon (Si) element, which denotes the presence of M-SiO_2 in PEGM-SiO_2 composites, was also discovered in addition to the elements identified in pure epoxy resin.

The presence of Si particles in PEGM-SiO_2 composites was confirmed by SEM mapping analysis. The presence of C, O, and Si particles in the PEGM-SiO_2 composite structure can be seen in Fig. 5. These results showed that M-SiO_2 was distributed homogeneously in the epoxy composite and there was no agglomeration. The most striking points are the homogeneous distribution of the obtained M-SiO_2 particles in the material and the absence of agglomeration.

Fig. 6a–c shows the tensile test results for elongation at break, tensile strength, and tensile modulus. The figure illustrates that the addition of M-SiO_2 to epoxy resin resulted in an improvement in its tensile strength. The epoxy resin tensile strength of 54.66 MPa was obtained as 57.61, 57.65, and 59.42 MPa for PEG2M-SiO_2, PEG6M-SiO_2, and PEG35M-SiO_2 composites, respectively. Compared to pure epoxy resin, the tensile strength of PEG2M-SiO_2, PEG6M-SiO_2, and PEG35M-SiO_2 composites increased by 5.3%, 5.4%, and 8.7%, respectively. Additionally, it was found that there was an increase in the tensile modulus as the pore diameter increased (Fig. 6-b). The tensile modulus of pure epoxy resin is 1096 MPa, and this value was obtained as 1207 MPa, 1261 MPa, and 1352 MPa for PEG2M-SiO_2, PEG6M-SiO_2, and PEG35M-SiO_2 composites, respectively. The tensile modulus of PEG2M-SiO_2, PEG6M-SiO_2 and PEG35M-SiO_2 composites increased by 10.1%, 15.0% and 23.3% respectively, compared to epoxy resin. The increase in tensile modulus of epoxy/M-SiO_2 composite samples is also attributed to the better distribution of M-SiO_2 in the epoxy resin. The strong load-bearing capability of M-SiO_2 and consequent improvement in its tensile modulus may have resulted from the strong adhesion between M-SiO_2 and epoxy resin. This outcome is consistent with previous research by Al-Namie et al. (Al Namie et al., 2011), who found that adding 40 wt % silica or 40 wt % alumina to the matrix increased the tensile modulus of epoxy by up to 145% and 182%, respectively. In addition, the higher surface area of M-SiO_2 gives better adhesion in epoxy, thus forming a stiffer material, which is attributed to the higher modulus. The variation of % elongation values according to M-SiO_2 pore diameter was given in Fig. 6-c. The addition of M-SiO_2 significantly reduced the elongation at break values of epoxy resin, which has low elongation at break. It reduced the elongation at break of the PEG35M-SiO_2 composite sample by 5.1% compared to the pure epoxy resin. When the tensile test results are evaluated, the highest mechanical properties found in the PEG35M-SiO_2 composite may be connected to the characteristics of the additional M-SiO_2. Although all three M-SiO_2 additive materials are seen to be amorphous in the XRD diffraction patterns, it can be seen that PEG35M-SiO_2 has a more crystalline structure compared to PEG2M-SiO_2 and PEG6M-SiO_2 composites. Furthermore, the SiO_2 peak of the PEG2M-SiO_2 composite was found to be more prominent in the FT-IR analysis compared to the PEG6M-SiO_2 and PEG35M-SiO_2 composites. This is an indication that M-SiO_2 particles are less homogeneously mixed in the epoxy matrix, and this result is supported by tensile tests. The agglomeration of M-SiO_2 in the PEG2M-SiO_2 composite reduced the

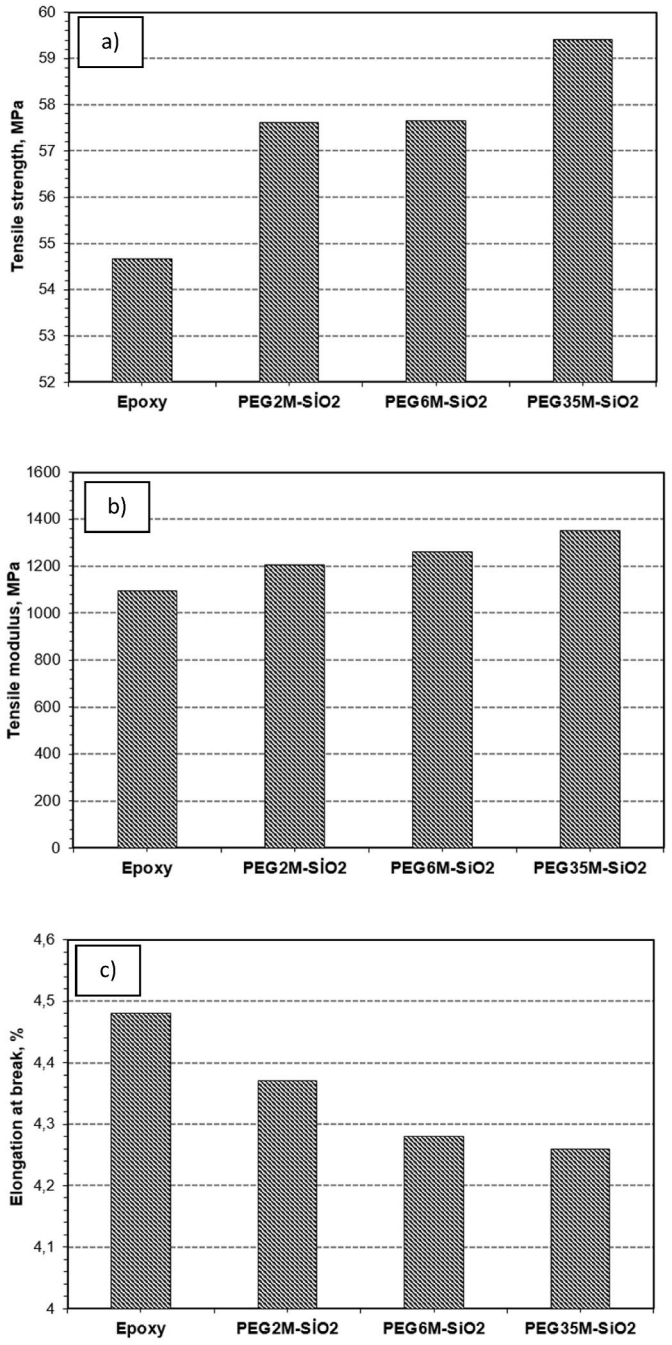


Fig. 6. Tensile strength, tensile modulus, and elongation at break of Epoxy and Epoxy/PEG_xM-SiO_2 composites.

mechanical properties.

4. Conclusion

It was observed that all three M-SiO_2s prepared by XRD were amorphic in structure, however, the M-SiO_2 obtained from PEG35000 was more crystalline than the others. According to the FT-IR spectra, it indicates that the prepared M-SiO_2 is distributed homogeneously in the epoxy; therefore, although the ratio of M-SiO_2 in the epoxy is 10%, the characteristic peaks of silica are distributed homogeneously in the composite. By EDS analysis, the presence of silicon in PEG2M-SiO_2, PEG6M-SiO_2, and PEG35M-SiO_2 composites was detected and distributed homogeneously in the matrix.

After being mixed with epoxy resin, the tensile strength of the M-SiO_2, PEG2M-SiO_2, PEG6M-SiO_2, and PEG35M-SiO_2 composites increased by 5.3%, 5.4%, and 8.7%, respectively. In comparison to pure epoxy, the tensile modulus of PEG2M-SiO_2, PEG6M-SiO_2 and PEG35M-SiO_2 composites increased by 10.1%, 15.0% and 23.3% respectively.

References

Al Namie, I., Ibrahim, A. A., & Hassan, M. F. (2011). Study the Mechanical properties of epoxy resin reinforced with silica (quartz) and alumina particles. *The Iraqi Journal For Mechanical And Material Engineering, 11*, 3.

Centi, G., Perathoner, S., Anderson, J. A., Castaldi, M. J., Centi, G., Perathoner, S., & White, M. (2009). Nano-architecture and reactivity of titania catalytic materials. Part 2. Bidimensional nanostructured films. In J. J. Spivey, & K. M. Dooley (Eds.), *Catalysis*, 21, pp. 0.

Cheng, C.-F., Cheng, H.-H., Cheng, P.-W., & Lee, Y.-J. (2006). Effect of reactive channel functional groups and nanoporosity of nanoscale mesoporous silica on properties of polyimide composite. *Macromolecules, 39*(22), 7583–7590. https://doi.org/10.1021/ma060990u

Dubey, R. S., Rajesh, Y. B. R. D., & More, M. A. (2015). Synthesis and characterization of SiO2 nanoparticles via sol-gel method for industrial applications. *Materials Today: Proceedings, 2*(4), 3575–3579. https://doi.org/10.1016/j.matpr.2015.07.098

Fowler, C. E., Khushalani, D., Lebeau, B., & Mann, S. (2001). Nanoscale materials with mesostructured interiors. *Advanced Materials, 13*(9), 649–652. https://doi.org/10.1002/1521-4095(200105)13:9<649::AID-ADMA649>3.0.CO;2-G

Fu, S.-Y., Feng, X.-Q., Lauke, B., & Mai, Y.-W. (2008). Effects of particle size, particle/matrix interface adhesion and particle loading on mechanical properties of particulate–polymer composites. *Composites Part B: Engineering, 39*(6), 933–961. https://doi.org/10.1016/j.compositesb.2008.01.002

Hussain, F., Hojjati, M., Okamoto, M., & Gorga, R. E. (2006). Review article: Polymer-matrix nanocomposites, processing, manufacturing, and application: An overview. *Journal of Composite Materials, 40*(17), 1511–1575. https://doi.org/10.1177/0021998306067321

Kalita, P., & Kumar, R. (2007). Ce-Al-MCM-41: An efficient catalyst for mukaiyama-michael reaction. *Studies in Surface Science and Catalysis, 170*, 1161–1166. https://doi.org/10.1016/S0167-2991(07)80973-6

Kango, S., Kalia, S., Celli, A., Njuguna, J., Habibi, Y., & Kumar, R. (2013). Surface modification of inorganic nanoparticles for development of organic–inorganic nanocomposites—a review. *Progress in Polymer Science, 38*(8), 1232–1261. https://doi.org/10.1016/j.progpolymsci.2013.02.003

Liu, H., Lao, Y., Wang, J., Jiang, J., Yu, C., & Liu, Y. (2022). Rational design of mesoporous silica (SBA-15)/PF (phenolic resin) nanocomposites by tuning the pore sizes of mesoporous silica. *Materials, 15*(24), 8879. https://doi.org/10.3390/ma15248879

Nooney, R. I., Thirunavukkarasu, D., Chen, Y., Josephs, R., & Ostafin, A. E. (2002). Synthesis of nanoscale mesoporous silica spheres with controlled particle size. *Chemistry of Materials, 14*(11), 4721–4728. https://doi.org/10.1021/cm0204371

Shiju, N. R., Alberts, A. H., Khalid, S., Brown, D. R., & Rothenberg, G. (2011). Mesoporous silica with site-isolated amine and phosphotungstic acid groups: A solid catalyst with tunable antagonistic functions for one-pot tandem reactions. *Angewandte Chemie International Edition, 50*(41), 9615–9619. https://doi.org/10.1002/anie.201101449

Suzuki, N., Kiba, S., Kamachi, Y., Miyamoto, N., & Yamauchi, Y. (2011). Mesoporous silica as smart inorganic filler: Preparation of robust silicone rubber with low thermal expansion property. *Journal of Materials Chemistry, 21*(14), 5338–5344. https://doi.org/10.1039/C0JM03767B

Suzuki, N., Kiba, S., & Yamauchi, Y. (2011). Fabrication of mesoporous silica/polymer composites through solvent evaporation process and investigation of their excellent low thermal expansion property. *Physical Chemistry Chemical Physics, 13*(11), 4957–4962. https://doi.org/10.1039/C0CP02071K

Ulusal, F. (2024). The synthesis and cytotoxicity analysis of gold nanoparticles coated with mesoporous SiO2 from gold treatment wastewater for medical applications. *Inorganic Chemistry Communications, 159*, Article 111867. https://doi.org/10.1016/j.inoche.2023.111867

Vaia, R. A., & Maguire, J. F. (2007). Polymer nanocomposites with prescribed morphology: Going beyond nanoparticle-filled polymers. *Chemistry of Materials, 19*(11), 2736–2751. https://doi.org/10.1021/cm062693+

Yoshina-Ishii, C., Asefa, T., Coombs, N., MacLachlan, M. J., & Ozin, G. A. (1999). Periodic mesoporous organosilicas, PMOs: Fusion of organic and inorganic chemistry 'inside' the channel walls of hexagonal mesoporous silica. *Chemical Communications*, (24), 2539–2540. https://doi.org/10.1039/A908252B

Zhang, F.-A., Lee, D.-K., & Pinnavaia, T. J. (2010). PMMA/mesoporous silica nanocomposites: Effect of framework structure and pore size on thermomechanical properties. *Polymer Chemistry, 1*(1), 107–113. https://doi.org/10.1039/B9PY00232D

Zhao, D., Feng, J., Huo, Q., Melosh, N., Fredrickson, G. H., Chmelka, B. F., & Stucky, G. D. (1998). Triblock copolymer syntheses of mesoporous silica with periodic 50 to 300 angstrom pores. *Science, 279*(5350), 548–552. https://doi.org/10.1126/science.279.5350.548